In Vivo Effect of Mutant ELOVL4 on the Expression and Function of Wild-Type ELOVL4

Nawajes A. Mandal,[1–4] Julie-Thu A. Tran,[1,4] Lixin Zheng,[1,4] Joseph L. Wilkerson,[4,5] Richard S. Brush,[1,4] Joel McRae,[1,4] Martin-Paul Agbaga,[1,4] Kang Zhang,[6] Konstantin Petrukhin,[7] Radha Ayyagari,[6] and Robert E. Anderson[1,4,5]

[1]Department of Ophthalmology, University of Oklahoma Health Sciences Center, Oklahoma City, Oklahoma, United States
[2]Department of Physiology, University of Oklahoma Health Sciences Center, Oklahoma City, Oklahoma, United States
[3]Oklahoma Center for Neuroscience, University of Oklahoma Health Sciences Center, Oklahoma City, Oklahoma, United States
[4]Dean McGee Eye Institute, Oklahoma City, Oklahoma, United States
[5]Department of Cell Biology, University of Oklahoma Health Sciences Center, Oklahoma City, Oklahoma, United States
[6]Shiley Eye Center, University of California San Diego, Jacobs Retina Center, San Diego, California, United States
[7]Department of Ophthalmology, Columbia University, New York, New York, United States

Correspondence: Nawajes A. Mandal, Department of Ophthalmology, University of Oklahoma Health Sciences Center, 608 Stanton L. Young Boulevard, Oklahoma City, OK 73104, USA; mmandal@ouhsc.edu.

Submitted: September 4, 2013
Accepted: March 3, 2014

Citation: Mandal NA, Tran J-TA, Zheng L, et al. In vivo effect of mutant ELOVL4 on the expression and function of wild-type ELOVL4. *Invest Ophthalmol Vis Sci*. 2014;55:2705–2713. DOI:10.1167/iovs.13-13198

Purpose. Mutations in the *elongation of very long chain fatty acids 4* (*ELOVL4*) gene cause human Stargardt's macular dystrophy 3 (STGD3), a juvenile onset dominant form of macular degeneration. To understand the role of the ELOVL4 protein in retinal function, several mouse models have been developed by using transgenic (TG), knock-in ($Elovl4^{+/mut}$), and knockout ($Elovl4^{+/-}$) approaches. Here we analyzed quantitatively the ELOVL4 protein and its enzymatic products (very long chain saturated fatty acid [VLC-FA] and VLC–polyunsaturated fatty acid [VLC-PUFA]) in the retinas of 8 to 10-week-old $TG1^+$, $TG2^+$, and $Elovl4^{+/mut}$ mice that harbor the mutant ELOVL4 and compared them to their wild-type littermates and $Elovl4^{+/-}$ that do not express the mutant protein. We also analyzed skin from these mice to gain insight into the pathogenesis resulting from the *ELOVL4* mutation.

Methods. ELOVL4 protein localization in the retina was determined by immunohistochemistry. Levels of wild-type ELOVL4 protein in skin and retinas were determined by Western blotting. Total lipids from skin and retinas were measured by gas chromatography–mass spectrometry (GC-MS). Retinal glycerophosphatidylcholines (PC) were analyzed by tandem mass spectrometry.

Results. Immunohistochemical and Western analysis indicated that wild-type ELOVL4 protein was reduced in heterozygous $Elovl4^{+/mut}$ and $Elovl4^{+/-}$ retinas, but not in $TG2^+$ retinas. We found that VLC-FA was reduced by 50% in the skin of $Elovl4^{+/-}$ and by 60% to 65% in $Elovl4^{+/mut}$. We found VLC-PUFA levels at ~50% in both the retinas, and wild-type levels of VLC-PUFA in $TG2^+$ retinas.

Conclusions. We conclude that the presence of the mutant ELOVL4 does not affect the function of wild-type ELOVL4 in the fully developed 8- to 10-week-old retinas.

Keywords: ELOVL4, VLC-PUFA, retina

Mutations in the *elongation of very long chain fatty acids 4* (*ELOVL4*) gene cause a juvenile onset dominant macular degeneration in humans called Stargardt's macular dystrophy 3 (STGD3). The ELOVL4 protein is a component of the fatty acid elongation system, which catalyzes a condensation reaction, the first and rate limiting step in fatty acid elongation,[1] and is specific for the production of very long chain saturated (VLC-FA) and polyunsaturated fatty acids (VLC-PUFA) greater than 26 carbons.[1] The last five amino acids of the C-terminal end of the ELOVL4 protein contains an endoplasmic reticulum (ER) retention signal (KXKXX), and all known mutations cause deletion of this signal.[2–4] As a result, the mutant protein loses its ER retention/retrieval signal and hence cannot be localized to the ER, the site for its involvement in fatty acid elongation. In cell culture, the ELOVL4 protein may exist as a multi-subunit complex with three other enzymes involved with subsequent steps in the addition of two carbon units,[5] and interactions of mutant and wild-type (WT) ELOVL4 have been demonstrated.[5,6] In studies with cultured cells that express both mutant and wild-type ELOVL4, the wild-type protein was found to be associated with the mutant protein and located in a juxtanuclear region.[5–8]

The phenotype of STGD3 could therefore be a result of any of the following scenarios, which may not be mutually exclusive: (1) the mislocalization of mutant proteins followed by aggregation in the inner segment, which mediates photoreceptor cell death; (2) the binding of mutant and WT proteins leading to the mislocalization of the WT protein, reducing the quantity of functional ELOVL4 in the ER, which causes a reduction of the products (VLC-PUFA) required for photoreceptor survival; (3) the production of toxic 3-keto-intermediate products by the mutant protein due to its separation from the ER (home of other enzymes involved in 2-carbon elongation); (4) the misdirection of the mutant protein to the photoreceptor

outer segment membranes and ultimately to the RPE, which may induce cellular stress; or (5) a dominant negative effect of mutant protein on WT enzymatic activity, which would lead to lower than expected (50% of WT) VLC-PUFA levels in the retina. Our ongoing studies and some recent publications provide significant leads to better understand ELOVL4 function; however, much remains to be learned.

In the past 10 years, various *Elovl4* mouse models have been developed that include knockout (*Elovl4*$^{+/-}$),[9] knock-in (*Elovl4*$^{+/mut}$),[10,11] conditional knockouts,[12] and transgenic (TG) models.[6] Homozygous *Elovl4*$^{mut/mut}$ and *Elovl4*$^{-/-}$ pups do not survive beyond a few hours of birth due to the loss of skin permeability barrier function, which is formed by sphingolipids containing VLC-FAs (≥C28).[10,13–15] Retinal phenotypes were characterized in heterozygous mice in both models. The *Elovl4*$^{+/-}$ retina, which supposedly has 50% of functional ELOVL4, was structurally and functionally no different from WT retina, indicating that a 50% reduction (haplo-insufficiency) does not affect retinal structure and function.[9,13] On the other hand, *Elovl4*$^{+/mut}$, which is genetically similar to human STGD3 patients, demonstrates retinal phenotypes, although mild, such as a slow degeneration of photoreceptors and accumulation of lipofuscin-like materials in the RPE.[10,11,16] The TG mouse lines developed by Karan et al.[6] express different levels of the human mutant *ELOVL4* gene in photoreceptor cells. These mice had a retinal phenotype closely resembling human STGD3 with accumulation of undigested phagosomes and lipofuscin in their RPE, which caused RPE atrophy and subsequent photoreceptor degeneration in the central retina.[6] The degree of severity of the pathological outcome varied with the level of mutant gene expression, such that the higher the expression level the more severe the phenotype.[6] Here we performed a comparative study on the expression of the ELOVL4 protein and the levels of VLC-PUFA (the products of ELOVL4) were compared in the fully developed retinas (8 to 10 weeks old) of these transgenic mouse lines (*Elovl4*$^{+/-}$, *Elovl4*$^{+/mut}$, TG1^{+}, TG2^{+}, and WT1^{+}; the nomenclature of the TG mice are as reported by Karan et al.[6]) in order to understand how the presence of a mutant protein in the retina induces pathology. Our side-by-side comparison of ELOVL4 products in *Elovl4*$^{+/-}$, *Elovl4*$^{+/mut}$, and TG2^{+} retinas provides some insightful information on how mutant ELOVL4 interacts with and affects the function of wild-type ELOVL4 in vivo.

Materials and Methods

Animal and Tissue Collection

The *Elovl4*$^{+/mut}$ line we used was generated by Rhada Ayyagari at the University of Michigan[11,16] and the *Elovl4*$^{+/-}$ line by Konstantine Petrukhin at Merck Research Laboratories.[9] We used transgenic mice generated by Karan et al.[6] and provided by Kang Zhang that express the human mutant ELOVL4 (TG1^{+} and TG2^{+}) and human wild-type *ELOVL4* genes (WT1^{+}), and their no-transgene-carrying wild-type littermates (WT1^{-}, TG1^{-}, and TG2^{-}) in a C57BL/6J background. Mice were born and raised in the OUHSC Rodent Barrier Facility and maintained under dim cyclic light (50 lux, 12 hours on/off, 7AM–7 PM). At age 8 to 10 weeks, retinal and eyecup tissues were harvested after overnight dark adaptation, quick frozen in liquid nitrogen, and stored at –80°C until used for analysis. We also collected tail tips of the mice (3–4 mm) to isolate skin proteins and whole-body skin for lipid analysis. Animals were cared for and handled according to the ARVO Statement for the Use of Animals in Vision and Ophthalmic Research. All protocols were approved by the Institutional Animal Care and Use Committee (IACUC) and comply with the guidelines of the University of Oklahoma Health Sciences Center and the Dean McGee Eye Institute for use of animals in research.

Immunohistochemistry

Mouse retinas were processed for cryosectioning as described earlier.[1] After blocking with 10% horse serum, the sections were incubated overnight at 4°C with ELOVL4 antibodies (1:200).[1] Sections were washed with PBS and labeled for 1 hour with AlexaFluor 488 conjugated chicken anti-rabbit secondary antibody (1:2000; Invitrogen, Carlsbad, CA, USA). Images were captured with an confocal microscope (Olympus FluoView FV500; Olympus Corp., Tokyo, Japan). For a comparative analysis, we kept all microscopic and capturing parameters the same for wild-type and mutant samples.

Quantitative Western Blotting

Tissue protein was extracted in T-PER reagent (Pierce Biotechnology, Rockford, IL) containing complete protease inhibitors (Roche Applied Science, Indianapolis, IN, USA). Protein concentration was determined using a commercial reagent (BCA Reagent; Pierce Biotechnology). Equal amounts of protein (30 μg) were separated on 10% polyacrylamide gels. Western hybridization with rabbit polyclonal ELOVL4 antibody (1:1000)[1] and mouse monoclonal β-actin antibody (Abcam, Cambridge, MA, USA) was done following a previously published protocol.[1] Chemiluminescence was developed using a Western blotting substrate (Super-Signal West Dura Extended Duration Substrate; Pierce Biotechnology) with a digital imaging system (IS4000R; Kodak, New Haven, CT, USA). The intensities of protein bands were determined using Java-based imaging software (ImageJ 1.32j; National Institutes of Health, Bethesda, MD, USA). Care was taken to ensure that the digitized bands were not saturated.

Fatty Acid Extraction and Analysis

Short and long-chain fatty acids were analyzed using GC-FID and GC-MS procedures as described earlier.[1,17] Total lipids were extracted from mouse retinas using the Bligh–Dyer method[18] with minor modifications as described previously by Martin et al.[19] and from skin using the method of Folch et al.[20] Fatty acid methyl esters (FAMES) were prepared from total lipid extracts by subjecting them to strong acid hydrolysis (16.6% HCl in methanol) at 75°C overnight and analyzed as described previously.[1,17] Retinal phosphatidylcholines (PCs) were further analyzed by tandem mass spectrometry by methods described previously.[21] Briefly, one mouse retina per sample was homogenized in 40% aqueous methanol and then diluted (1:40) with 2-propanol/methanol/chloroform (4:2:1 vol/vol/vol) containing 20 mM ammonium formate and 1.00 μM PC 14:0/14:0 (as internal standard). Samples were introduced into a triple quadrupole mass spectrometer (TSQ Ultra; Thermo Fisher Scientific, Inc., Rockville, MD, USA) using a chip-based nano-ESI source (NanoMate; Advion, Inc., Ithaca, NY, USA) operating in infusion mode. Commercial software (Chipsoft; Advion, Inc.) was used to set the device's spray voltage to 1.4 kV and the gas pressure to 0.6 psi. The ion transfer tube of the mass spectrometer was maintained at 200°C. Tandem mass spectrometry (MS/MS) spectra were acquired at a rate of 500 *m/z* per second by methods created using data analysis software (XCalibur; Thermo Fisher Scientific, Inc.). Phosphatidylcholines were identified by using precursor ion (PI) scanning of *m/z* 184. The isolation windows of quadrupoles 1 and 3 were maintained at 0.5 Da, while the collision gas pressure of quadrupole 2 was maintained at 0.5 mTorr of

argon. Automated peak finding, correction for 13C isotope effects, and quantitation of lipid molecular species against internal standard (PC 14:0/14:0) were performed using the lipid mass spectrum analysis (LIMSA) software peak model fit algorithm. All species of retinal PC containing VLC-PUFA are presented as % PC (relative percent of the total PC species detected).

Statistical Analysis

Quantitative data are expressed as mean ± SD for each group. Statistical analyses were performed using statistical and analytics software (Statistica 64; Statsoft, Inc., Tulsa, OK, USA). The Student's *t*-test and one-way ANOVA with post hoc Scheffe was utilized to assess statistical significance.

Results

Immunohistochemical Evaluation of ELOVL4 Proteins in the Retina

In mouse and rat tissues, ELOVL4 is highly expressed in the retina, the only tissue known to be affected by the dominant heterozygous mutations in humans.[1,22] In mammals, ELOVL4 localizes to the cytoplasmic ER of both rod and cone photoreceptor cells.[5,23,24] Using an antibody that recognizes the wild-type ELOVL4 but not the mutant ELOVL4 protein,[1] we detected expression of the protein in the retina of the different transgenic mice. When we compared wild-type and heterozygous *Elovl4*$^{+/-}$ and *Elovl4*$^{+/mut}$ littermates for ELOVL4 labeling, we observed a substantial reduction of ELOVL4 signal in the heterozygous retinas (Fig. 1; compare 1A with 1B, and 1C with 1D). Although not quantitative, these data support a reduction of wild-type ELOVL4 protein in heterozygous retinas. At the same time, we did not detect any noticeable difference in localization of wild-type ELOVL4 proteins between *Elovl4*$^{+/mut}$ and *Elovl4*$^{+/-}$ retinas (Figs. 1B, 1D). The labeling intensity of wild-type ELOVL4 was not changed in TG2^{+} retinas, although the photoreceptor cell loss was prominent in TG2^{+} retinas at this stage (10-week old mice), as shown by the reduction of outer nuclear layer (ONL) thickness (Fig. 1F).

Quantitation of ELOVL4 Protein

In the *Elovl4*$^{+/-}$ and *Elovl4*$^{+/mut}$ lines, the quantity of wild-type ELOVL4 protein was expected to be 50% of the WT. The antibody we used can detect monomeric ELOVL4 from an unboiled sample. In the retina, the quantity of ELOVL4 monomer in *Elovl4*$^{+/-}$ appears to be 28% to 40% of that obtained for wild-type littermates (mean: 37%; $n = 5$; Figs. 2A, 2B). On the other hand, the levels of ELOVL4 wild-type monomer in the *Elovl4*$^{+/mut}$ ranged from 18% to 38% of that obtained for littermate wild-types with a mean value of 28% ($n = 8$; Figs. 2A, 2B). In the skin, we found the amount of ELOVL4 monomer (percent of control levels) to be 37% in *Elovl4*$^{+/-}$ and 20% in *Elovl4*$^{+/mut}$ (Figs. 2C, 2D). The ELOVL4 protein can dimerize and mutant ELOVL4 can bind to wild-type ELOVL4 in vitro and in transient transfection assays.[5,8,25] It was predicted that wild-type and mutant ELOVL4 could potentially associate in the mouse retina, and this association could lead to protein accumulation in undesired cellular compartments and ultimately to proteosomal degradation of both the mutant and wild-type proteins.[8,25] This could explain a higher level of reduction of wild-type ELOVL4 in *Elovl4*$^{+/mut}$ tissues (Figs. 2C, 2D). However, we did not find any difference in the level of wild-type protein in the retinas of the TG lines (Fig. 2E). This may suggest that the human mutant ELOVL4 expressed from interphotoreceptor retinoid–binding protein promoter in transgenic retinas does not interact with endogenous mouse wild-type ELOVL4. These data also suggest that the expression of the transgenic *ELOVL4* did not affect the expression of endogenous *Elovl4* in the TG lines.

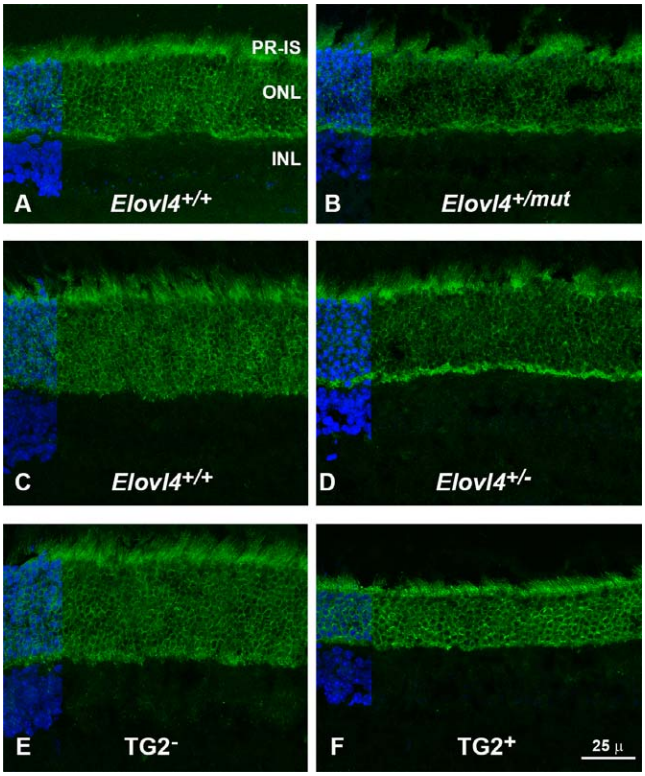

Figure 1. Immunohistochemical labeling of ELOVL4 protein in *Elovl4* knock-in, knockout, and TG2^{+} mouse retinas. Eight- to 10-week-old mouse eyes from the mutant *Elovl4* lines, knock-in (**B**), knockout (**D**), and TG2^{+} (**F**), and their corresponding littermate wild-types in figures (**A**), (**C**), and (**E**), respectively, were fixed for cryosectioning and labeled with rabbit polyclonal anti-ELOVL4 antibody. Perinuclear and inner segment labeling of ELOVL4 in photoreceptor cells was noted in all the genotypes. PR-IS, photoreceptor inner segment; INL, inner nuclear layer.

Quantitation of the ELOVL4 Products VLC-PUFA and VLC-FA

ELOVL4 is an enzyme that elongates both saturated and polyunsaturated fatty acids from 26 carbons to longer carbon chains.[1] Very long chain saturated fatty acids (saturated) are an important component of skin acyl ceramides, which form highly ordered lamellar membranes in the epidermis and provide the skin water permeability barrier.[15] However, they are not a major constituent of retinal lipids, which has a significant presence of VLC-PUFA in its phospholipids, mainly in PC.[1,26] Very long chain polyunsaturated fatty acids are predicted to have a role in maintaining the structure of the photoreceptor outer segment discs and/or have a role in proper functioning of the phototransduction proteins in photoreceptor disc membranes.[27,28] Complete ablation of ELOVL4 protein in mice abolishes the production of fatty acids beyond C28 and longer,[14] indicating ELOVL4 is required for the synthesis of fatty acids up to and beyond C28 in length. In the Table, we presented all the fatty acid species from total lipids C14 through C24, which are not products of ELOVL4, from the heterozygous retinas of both *Elovl4*$^{+/-}$ and *Elovl4*$^{+/mut}$ mice along with their

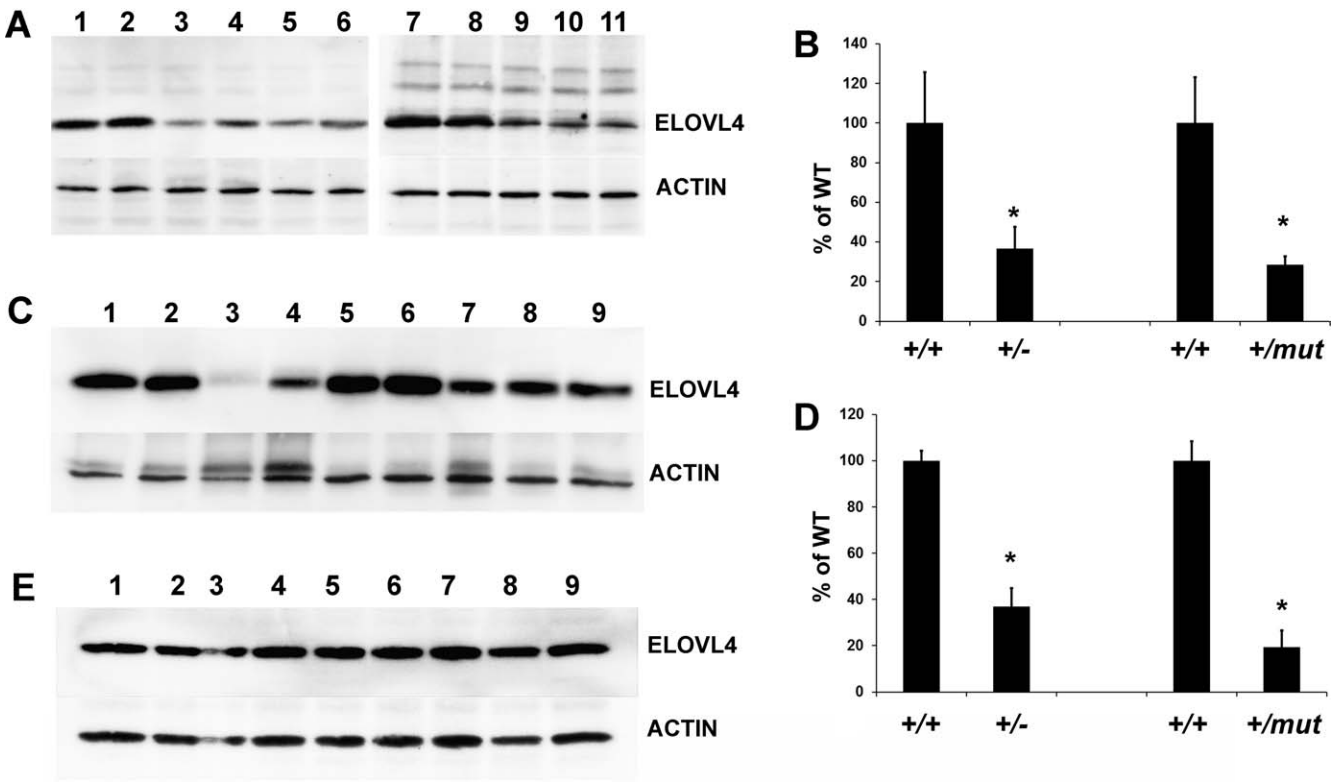

Figure 2. Western blot detection of ELOVL4 proteins in the retina and skin of *Elovl4* knock-in and knockout mice and in the retina of transgenic lines. (**A**) Lanes 1 to 2: $Elovl4^{+/+}$ littermates from knockout line; lanes 3 to 6: heterozygous littermates from knock-out line ($Elovl4^{+/-}$); lanes 7 to 8: wild-type littermates from knock-in line; lanes 9 to 11, heterozygous littermates from knock-in line ($Elovl4^{+/mut}$). (**B**) Densitometric quantification of ELOVL4 proteins from knock-in and knockout retina ($n = 6$–9; $^*P < 0.01$). Data presented as percentage of wild-type, which is 100%. (**C**) Western blot quantification of ELOVL4 proteins in knock-in and knockout skin. Representative Western blots; lanes 1 to 4: $Elovl4^{+/mut}$; lanes 5 to 6: $Elovl4^{+/+}$; lanes 7 to 9: $Elovl4^{+/-}$. (**D**) Densitometric quantification of ELOVL4 proteins in skin ($n = 4$; $^*P < 0.01$). Data presented as percentage of wild-type, which is 100%. (**E**) Western blot analysis of retinas from TG lines. Lanes 1 to 3: $TG1^+$; lanes 4 to 5: $TG2^+$; lanes 6 to 7: TG^-; and lanes 8 to 9: $WT1^+$, as originally described by Karan et al.[6]

Table. Fatty Acid Analysis of Retina From Elovl4 Knockout and Knock-in Mice

	$Elovl4^{+/+}$		$Elovl4^{+/mut}$		$Elovl4^{+/+}$		$Elovl4^{+/-}$	
Fatty Acid	**Mole, %**	**SD**	**Mole, %**	**SD**	**Mole, %**	**SD**	**Mole, %**	**SD**
14:0	0.26	0.02	0.32	0.06	0.29	0.03	0.33	0.08
16:0	24.17	2.51	23.91	0.42	23.78	0.63	24.68	1.31
16:1	0.55	0.15	0.76	0.17	0.81	0.10	0.84	0.11
18:0	23.44	2.59	21.77	0.61	22.40	0.63	22.25	0.62
18:1	8.68	0.77	9.62	0.69	9.65	0.29	9.69	0.18
18:2n6	0.88	0.12	0.92	0.02	1.00	0.11	1.15	0.10
20:0	0.39	0.14	0.39	0.13	0.33	0.04	0.35	0.06
20:1	0.31	0.02	0.33	0.06	0.30	0.02	0.28	0.02
20:5n3	0.30	0.07	0.28	0.04	0.26	0.07	0.23	0.03
20:2n6	0.32	0.02	0.31	0.01	0.33	0.02	0.31	0.01
20:3n6	0.44	0.03	0.46	0.01	0.45	0.06	0.45	0.06
20:4n6	5.38	0.44	5.68	0.55	6.03	0.53	5.80	0.50
22:0	0.24	0.11	0.28	0.13	0.21	0.04	0.24	0.06
22:4n6	0.75	0.04	0.75	0.05	0.75	0.09	0.73	0.07
22:5n6	0.09	0.01	0.09	0.01	0.11	0.01	0.10	0.01
22:5n3	0.88	0.08	0.81	0.02	0.67	0.05	0.65	0.06
22:6n3	30.77	4.03	31.57	0.89	30.55	0.78	30.20	1.29
24:0	0.14	0.06	0.16	0.08	0.12	0.02	0.14	0.03
24:1	0.11	0.02	0.13	0.04	0.10	0.01	0.10	0.01
24:5n3	0.40	0.03	0.40	0.02	0.37	0.03	0.37	0.03
24:6n3	0.82	0.05	0.65	0.04	0.82	0.04	0.72	0.03

All species of retinal fatty acids except VLC-PUFA are presented as relative mole percentage from four groups of mice: $Elovl4^{+/+}$ and $Elovl4^{+/mut}$ from the knock-in group, $Elovl4^{+/+}$ and $Elovl4^{+/-}$ from the knockout group. We did not find any significant changes in this group of fatty acids between heterozygous versus wild-type animals ($n = 6$ for all).

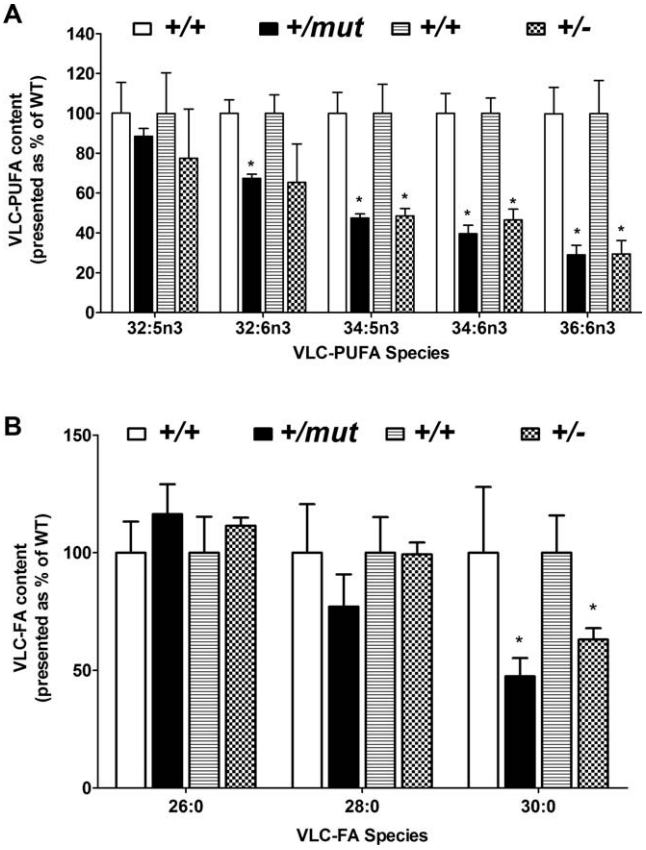

FIGURE 3. Fatty acid analysis of skin and retina from *Elovl4* knockout (*Elovl4*$^{+/-}$) and knock-in (*Elovl4*$^{+/mut}$) mice. (**A**) The relative mole percent values of VLC-PUFA species with carbon length > 30 were measured by GC-FID and are presented as a percentage of the wild-type, which is 100% ($n = 6$; $^*P < 0.01$). (**B**) Saturated very long chain fatty acids were analyzed in skin from adult mice by GC-MS and mole percent values of VLC-FA species are presented as a percentage of the wild-type, which is 100% ($n = 6$; $^*P < 0.01$).

wild-type littermates. Having only one normal copy of ELOVL4, these retinas had no significant difference in the levels of fatty acids below C28, which are not dependent on ELOVL4 activity, except for a slight decrease in 24:6n3 in both heterozygous groups (not statistically significant). However, the VLC-PUFA species were reduced significantly in the heterozygous animals, and the magnitude of reduction was increasingly higher as the carbon length increased, such that a ~30% reduction occurred in 32:6n3 and a ~70% reduction occurred in 36:6n3 (Fig. 3A). This clearly indicates that with one copy of ELOVL4, the efficiency of the enzyme decreases for each successive step in a stepwise addition of two carbons in the elongation scheme of VLC-PUFA synthesis. However, the pattern and the levels are not different between *Elovl4*$^{+/-}$ and *Elovl4*$^{+/mut}$ retinas at this age point (8–10 weeks old; Fig. 3A).

Because of the global nature of knock-in and knockout, we compared the skin of *Elovl4*$^{+/mut}$ and *Elovl4*$^{+/-}$ mice for VLC-FA in order to get another independent estimation of ELOVL4 activity. We detected a 53% reduction of the ELOVL4 product 30:0 (VLC-FA) in *Elovl4*$^{+/mut}$ skin and a 37% reduction in *Elovl4*$^{+/-}$ skin (Fig. 3B). We observed a 23% reduction in 28:0 levels in the *Elovl4*$^{+/mut}$ compared to wild-type, but no change in *Elovl4*$^{+/-}$ (Fig. 3B). In both heterozygous groups, the ELOVL4 substrate 26:0 was found to be increased by 11% to 16% compared with controls (Fig. 3B).

When we measured the fatty acid profile of TG lines, we found no difference in the levels of fatty acids that are not related to ELOVL4 activity (Fig. 4A). More particularly, the levels of docosahexaenoic acid (DHA, 22:6n3) and arachidonic acid (AA, 20:4n6) were not different among the different genotypes (Fig. 4A). Furthermore, no difference was found in the levels of VLC-PUFA in the retina in all the lines carrying transgenic proteins from their respective wild-type littermates, which are synthesized by ELOVL4 (Fig. 4B). These data indicate that in TG2$^+$ retinas the mutant transgenic ELOVL4 protein did not interfere with the enzymatic activity of the endogenous protein.

We further analyzed the PC species in all these retinas by tandem MS (Fig. 5). The result does not appear to be different from the VLC-PUFA fatty acid analysis of total retinal lipids. The VLC-PUFA containing PCs are significantly reduced (~50%) in both *Elovl4*$^{+/-}$ and *Elovl4*$^{+/mut}$ retinas compared with their wild-type littermates, and the level in *Elovl4*$^{+/mut}$ is not significantly different from the *Elovl4*$^{+/-}$ at this age point (Fig. 5). The VLC-PUFA containing PC species in TG2$^+$ retina are not different from their wild-type controls (Fig. 5). The levels of the PC species not containing VLC-PUFA were not different in the retinas in all the transgenic lines from the controls.

DISCUSSION

ELOVL4 is an essential protein required for synthesis of VLC-FA and VLC-PUFA. Mutations in this gene in humans lead to the development of STGD3 pathology, indicating that the presence of one mutant copy of the gene is sufficient to induce macular degeneration even in the presence of a normal copy. In mouse models like the *Elovl4*$^{+/-}$, where the mice have only one wild-type copy of ELOVL4, the retina appears normal.[9] However, when a mouse retina harbors the mutant ELOVL4, either from its own genome (such as *Elovl4*$^{+/mut}$) or from a transgene (TG1$^+$, TG2$^+$, TG3$^+$, as in transgenic lines developed by Karan et al.[6]), retinal pathology is induced.[11,16,29] This may indicate that the presence of the mutant ELOVL4 protein is responsible for RPE and photoreceptor cell death in STGD3. However, it is not known whether a reduction (of greater than 50%) of ELOVL4 function and thereby the amount of ELOVL4 products (VLC-FA and VLC-PUFA) is sufficient to induce photoreceptor and RPE cell death/dysfunction or if the presence of the mutant protein is necessary, or both. Since the mutant protein has been shown to interact with the wild-type protein in cultured cells,[7,8,25] there is a prediction that in tissues where both proteins are expressed, the binding of mutant ELOVL4 to the wild-type may either reduce its enzyme activity or make it partially unavailable for VLC-PUFA synthesis (the mutant protein does not have the ER retention signal). If the interaction stoichiometry between the wild-type and the mutant protein is 1:1, then only 25% of the ELOVL4 may be functional in human retinas as well as in *Elovl4*$^{+/mut}$ mice (25% of the dimers would have two wild-type proteins that would localize to the ER), and therefore only 25% VLC-PUFA would be synthesized in these retinas compared with controls. By analyzing the wild-type ELOVL4 protein and its product, we found in both retina and skin that the protein levels decreased and the magnitude of decrease is higher in the *Elovl4*$^{+/mut}$, suggesting the mutant protein may mislocalize a portion of wild-type protein (Fig. 2).

In *Elovl4*$^{+/-}$ mice, we expected to see a reduction in protein levels by 50%, but observed a reduction of 63%. It should be noted that the proteins were separated in an SDS-PAGE gel without heating or boiling (as boiling causes disruption of epitopes necessary for recognition by this

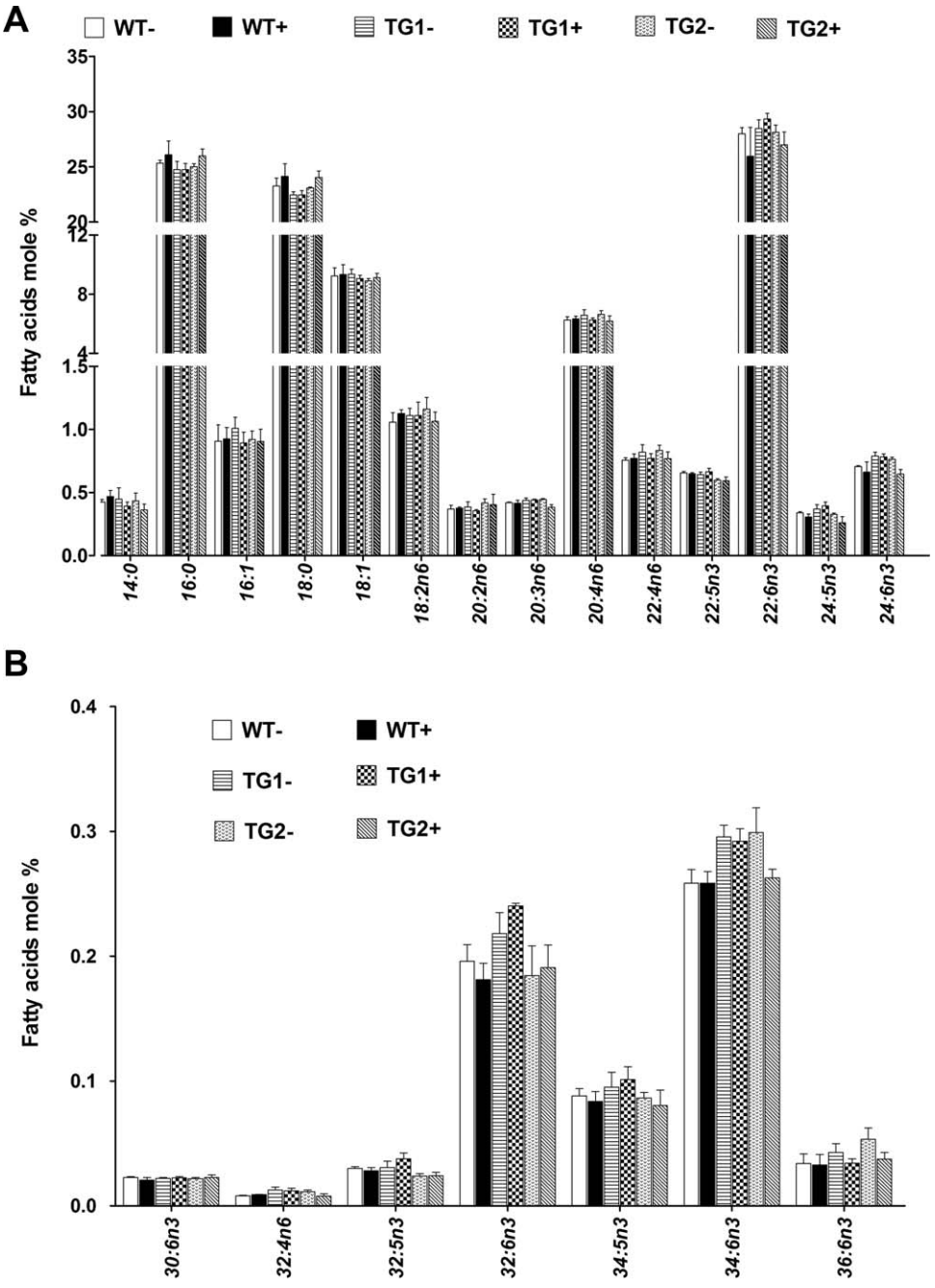

FIGURE 4. Fatty acid analysis of *Elovl4* transgenic retinas by GC-FID. (**A**) Fatty acid data presented as relative mole percentage from all the transgenic and control lines along with their littermates. (**B**) Very long chain polyunsaturated fatty acid composition as relative mole percentage. Data presented as mean ± SD ($n = 4$–6).

particular antibody) and quantification was done only for the monomeric forms. Therefore, the fraction of ELOVL4 present in higher order multimers or in membrane complexes is not accounted for in this quantification. If the amount of ELOVL4 in membrane complexes is similar in both heterozygous and wild-type tissues, the amount available for detection in the heterozygous is expected to be lower than 50% of the WT, which could be the reason for the 63% reduction in *Elovl4*$^{+/-}$. However, the reduction was greater in *Elovl4*$^{+/mut}$ mice where the wild-type protein levels were reduced by 72% to 80% compared with the wild-type (Fig. 2B). In *Elovl4*$^{+/mut}$ mice, the presence of only 20% to 28% monomeric wild-type protein indicates that the presence of the mutant protein has an effect on the wild-type protein. This may occur from the binding of mutant protein to wild-type protein, causing it to mislocalize and become a substrate by proteosomal degradation along with the mutant protein.

There are several interesting features of the fatty acid compositional data. First, there are no differences in the levels of DHA, the most abundant fatty acid in retinal lipids, in any of the retinas we examined. This is in sharp contrast to what we have previously reported for retinas from other mutant and transgenic rodent retinal degeneration models.[30,31] For example, retinas from P23H and S334ter rhodopsin mutant rats have lower DHA levels than their littermate controls.[31] Lines of P23H rats with the fastest rate of degeneration have lower

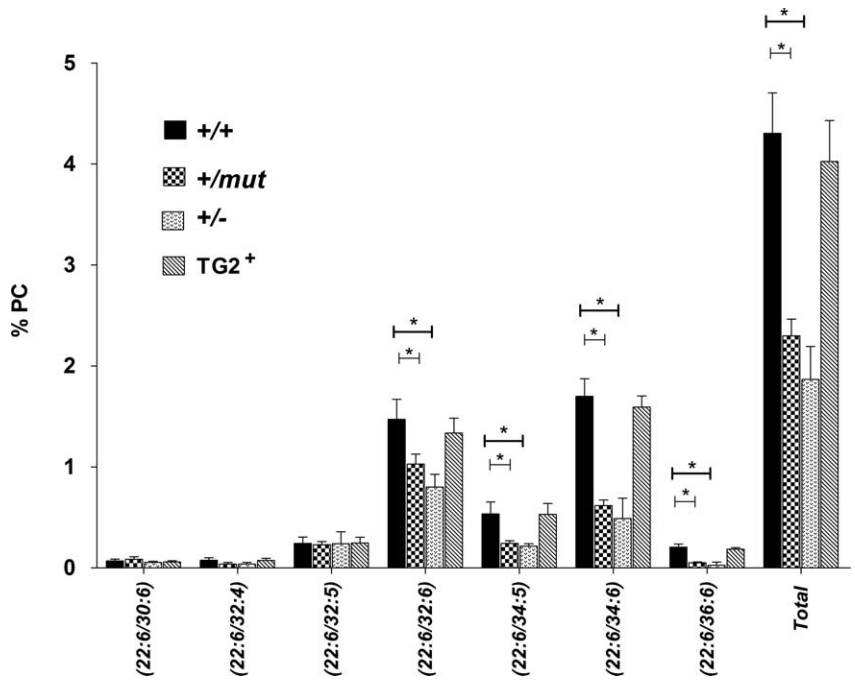

FIGURE 5. Tandem mass spectrometry analysis of retinal VLC-PUFA–containing PC lipid species. All species of retinal PC containing VLC-PUFA are presented as % PC (percent of the total PC species detected) from four groups of mice: *Elovl4*$^{+/mut}$, *Elovl4*$^{+/-}$, TG2^{+}, and controls (*Elovl4*$^{+/+}$; $n = 4$–14). The control values are derived from averaging the individual controls (wild-type littermates) from all three lines ($n = 4$–5 for each). $^{*}P < 0.05$.

levels of DHA compared with controls and those that degenerate slower. Mice with *Rds*[30] and *Rhodopsin* G90D[32] mutations have lower retinal DHA levels than appropriate controls. Of the various mutant rodent models we have analyzed, only those with ELOVL4 mutations or transgene expression of mutant protein, especially TG2^{+} retinas which undergo rapid degeneration, do not have lower retinal DHA levels. Second, although there were different levels of expression of wild-type *Elovl4* in *Elovl4*$^{+/-}$ and *Elovl4*$^{+/mut}$ mouse retina, the levels of VLC-PUFA were not different between the two groups at this age point, both having ~50% compared with controls. This reduction was expected, although we also expected a greater reduction in *Elovl4*$^{+/mut}$ retinas due to expression of the mutant protein. However, *Elovl4*$^{+/mut}$ skin appears to produce less VLC-FA, which are primarily found in ceramides, than *Elovl4*$^{+/-}$ skin (Fig. 3B). *Elovl4* is a high-expressing gene in the retina with expression levels 10- to 20-fold higher than in skin.[1,22] This is probably the reason that a small difference (10%) in the protein levels (enzyme activity) does not reflect a comparable difference in product levels in the retina between *Elovl4*$^{+/mut}$ and *Elovl4*$^{+/-}$, whereas the skin enzyme expression is not as abundant as in retina and thus their products are more affected. Several labs, including ours, showed a dominant negative effect of the mutant protein on the localization and function of wild-type protein in in vitro and cell culture studies.[7,8,25] It was surprising for us not to see a dominant negative effect of mutant ELOVL4 on the function of wild-type ELOVL4 in *Elovl4*$^{+/mut}$ retinas at this younger age. It will be interesting to follow this with age as the *Elovl4*$^{+/mut}$ mice are known to develop retinal pathology slowly and with aging.[11,16] Third, there was a progressive reduction in the formation of longer chain length VLC-PUFA in retinas of both *Elovl4*$^{+/-}$ and *Elovl4*$^{+/mut}$ mice (C32 > C34 > C36). The same was also noted in the skin profiles, where the levels of 30:0 were more affected than 28:0 in *Elovl4*$^{+/-}$ and *Elovl4*$^{+/mut}$ mice. This suggests that the enzyme activity of ELOVL4 is highly sensitive to the availability of substrates, which become more limited with increasing chain length. Fourth, the presumed expression of different levels of mutant human ELOVL4 in the TG mouse retinas (the mRNA levels were increased; however, there is no antibody to mutant human or mouse ELOVL4 so the level of protein expression cannot be determined) did not affect the retinal levels of VLC-PUFA (compare TG1^{+}, TG2^{+}, WT1^{+}, and TG^{-} in Fig. 4). This shows that the mutant human protein, if expressed, does not affect the enzymatic activity of the endogenous mouse ELOVL4. This conclusion is supported by the discussion above regarding the lack of an effect of mutant protein in *Elovl4*$^{+/mut}$ mice on levels of VLC-PUFA compared with *Elovl4*$^{+/-}$ retinas. This apparent lack of a dominant negative effect of mutant protein on the wild-type protein in mouse retinas raises questions and suggests that further studies are necessary to understand the mechanism of ELOVL4 mutation-mediated STGD3 in humans. Recent studies from our laboratory suggest that VLC-PUFA are important for rod function and survival, as we found that a reduction of VLC-PUFA (>90%) by conditionally deleting *Elovl4* in both rods and cones leads to a loss of rods at 6 months of age and a reduction in rod function (ERG) (Marchette LD, et al. *IOVS* 2012;53:ARVO E-Abstract 4654). Thus, the loss of VLC-PUFA could be a contributing factor since these mice do not express mutant ELOVL4, meaning the photoreceptor cell loss cannot be explained by the presence of mutant protein. This can explain the slower development of the mild phenotype in older *Elovl4*$^{+/mut}$ mice; the efficiency of ELOVL4 synthesis may go down with aging, which may result in a reduction in the VLC-PUFA levels in these retinas, contributing to the rod cell loss and loss of rod function.[10,11] However, it does not explain a dominant early onset human STGD3 development.

Other experiments from our lab showed that, in *Xenopus laevis*, the mutant mouse ELOVL4 protein mislocalizes to the photoreceptor outer segment (Agbaga M-P, et al. *IOVS* 2011;52:ARVO E-Abstract 1368), which can eventually be taken up by the RPE cells. In TG2^{+} mice, prominent RPE

atrophy was noted in aged mice, a significantly higher quantity of undigested phagosomes were seen in younger mice, and a loss of photoreceptor cells was noted as early as 2 months.[6] ELOVL4 protein levels, as well as the levels of VLC-PUFA, are not reduced in TG2^{+} retinas (Fig. 2E), and thus the reduction of VLC-PUFA is likely not the cause of photoreceptor cell death in this line, further supporting the notion that the presence of mutant protein in some undesired location may be toxic. Further, the severity in retinal pathology in TG mice has been found to be associated with the number of copies of the mutant ELOVL4 protein, with severity increasing with the increase of mutant expression.[6] In that comparison, *Elovl4*$^{+/mut}$ express one copy of the mutant ELOVL4, whereas TG2^{+} express greater than three copies, which could explain the milder phenotype of *Elovl4*$^{+/mut}$. In order to make comparisons to the human disease condition, the genetic makeup of the *Elovl4*$^{+/mut}$ mice was designed to mimic that of the human, although no early onset RPE atrophy is reported in these mice; however, since RPE cell loss is not localized to a specific region like the macula in humans, further investigation is needed. The toxic effect of the mutant ELOVL4 protein to the RPE cell has not been studied yet and is a potential area to explore as STGD3 mutation could potentially be affecting the RPE cells, causing RPE atrophy followed by photoreceptor cell death.

Acknowledgments

We thank Mark Dittmar (Dean A. McGee Eye Institute, Oklahoma City, Oklahoma, United States) for his assistance with animal breeding and feeding and Kevin Li, Abul K. Rahman, Louisa J. Williams, and Linda S. Boone (Department of Ophthalmology, OUHSC and Dean A. McGee Eye Institute, Oklahoma City, Oklahoma, United States) for their assistance in tissue collection, preparation, and histology.

Supported by an OUHSC College of Medicine Alumni Association Grant (NAM); National Eye Institute Grants EY022071 (NAM); EY04149, EY021725 (REA); EY013198, EY021237 (RA); EY019861 (KP); National Center for Research Resources Grant RR17703 (REA); NIH Grants NS067594, NS074476 (KP); Research to Prevent Blindness, Inc.; and the Foundation Fighting Blindness (REA).

Disclosure: **N.A. Mandal**, None; **J.-T.A. Tran**, None; **L. Zheng**, None; **J.L. Wilkerson**, None; **R.S. Brush**, P; **J. McRae**, None; **M.-P. Agbaga**, P; **K. Zhang**, None; **K. Petrukhin**, None; **R. Ayyagari**, None; **R.E. Anderson**, P

References

1. Agbaga MP, Brush RS, Mandal MN, Henry K, Elliott MH, Anderson RE. Role of Stargardt-3 macular dystrophy protein (ELOVL4) in the biosynthesis of very long chain fatty acids. *Proc Natl Acad Sci U S A*. 2008;105:12843–12848.
2. Bernstein PS, Tammur J, Singh N, et al. Diverse macular dystrophy phenotype caused by a novel complex mutation in the ELOVL4 gene. *Invest Ophthalmol Vis Sci*. 2001;42:3331–3336.
3. Maugeri A, Meire F, Hoyng CB, et al. A novel mutation in the ELOVL4 gene causes autosomal dominant Stargardt-like macular dystrophy. *Invest Ophthalmol Vis Sci*. 2004;45:4263–4267.
4. Zhang K, Kniazeva M, Han M, et al. A 5-bp deletion in ELOVL4 is associated with two related forms of autosomal dominant macular dystrophy. *Nat Genet*. 2001;27:89–93.
5. Grayson C, Molday RS. Dominant negative mechanism underlies autosomal dominant Stargardt-like macular dystrophy linked to mutations in ELOVL4. *J Biol Chem*. 2005;280:32521–32530.
6. Karan G, Lillo C, Yang Z, et al. Lipofuscin accumulation, abnormal electrophysiology, and photoreceptor degeneration in mutant ELOVL4 transgenic mice: a model for macular degeneration. *Proc Natl Acad Sci U S A*. 2005;102:4164–4169.
7. Logan S, Agbaga MP, Chan MD, et al. Deciphering mutant ELOVL4 activity in autosomal-dominant Stargardt macular dystrophy. *Proc Natl Acad Sci U S A*. 2013;110:5446–5451.
8. Vasireddy V, Vijayasarathy C, Huang J, et al. Stargardt-like macular dystrophy protein ELOVL4 exerts a dominant negative effect by recruiting wild-type protein into aggresomes. *Mol Vis*. 2005;11:665–676.
9. Raz-Prag D, Ayyagari R, Fariss RN, et al. Haploinsufficiency is not the key mechanism of pathogenesis in a heterozygous Elovl4 knockout mouse model of STGD3 disease. *Invest Ophthalmol Vis Sci*. 2006;47:3603–3611.
10. McMahon A, Butovich IA, Mata NL, et al. Retinal pathology and skin barrier defect in mice carrying a Stargardt disease-3 mutation in elongase of very long chain fatty acids-4. *Mol Vis*. 2007;13:258–272.
11. Vasireddy V, Jablonski MM, Mandal MN, et al. Elovl4 5-bp-deletion knock-in mice develop progressive photoreceptor degeneration. *Invest Ophthalmol Vis Sci*. 2006;47:4558–4568.
12. Barabas P, Liu A, Xing W, et al. Role of ELOVL4 and very long-chain polyunsaturated fatty acids in mouse models of Stargardt type 3 retinal degeneration. *Proc Natl Acad Sci U S A*. 2013;110:5181–5186.
13. Cameron DJ, Tong Z, Yang Z, et al. Essential role of Elovl4 in very long chain fatty acid synthesis, skin permeability barrier function, and neonatal survival. *Int J Biol Sci*. 2007;3:111–119.
14. Vasireddy V, Uchida Y, Salem N Jr, et al. Loss of functional ELOVL4 depletes very long-chain fatty acids (> or = C28) and the unique omega-O-acylceramides in skin leading to neonatal death. *Hum Mol Genet*. 2007;16:471–482.
15. Uchida Y, Holleran WM. Omega-O-acylceramide, a lipid essential for mammalian survival. *J Dermatol Sci*. 2008;51:77–87.
16. Vasireddy V, Jablonski MM, Khan NW, et al. Elovl4 5-bp deletion knock-in mouse model for Stargardt-like macular degeneration demonstrates accumulation of ELOVL4 and lipofuscin. *Exp Eye Res*. 2009;89:905–912.
17. Yu M, Benham A, Logan S, et al. ELOVL4 protein preferentially elongates 20:5n3 to very long chain PUFAs over 20:4n6 and 22:6n3. *J Lipid Res*. 2012;53:494–504.
18. Bligh EG, Dyer WJ. A rapid method of total lipid extraction and purification. *Can J Biochem Physiol*. 1959;37:911–917.
19. Martin RE, Elliott MH, Brush RS, Anderson RE. Detailed characterization of the lipid composition of detergent-resistant membranes from photoreceptor rod outer segment membranes. *Invest Ophthalmol Vis Sci*. 2005;46:1147–1154.
20. Folch J, Lees M, Sloane Stanley GH. A simple method for the isolation and purification of total lipides from animal tissues. *J Biol Chem*. 1957;226:497–509.
21. Busik JV, Reid GE, Lydic TA. Global analysis of retina lipids by complementary precursor ion and neutral loss mode tandem mass spectrometry. *Methods Mol Biol*. 2009;579:33–70.
22. Mandal MN, Ambasudhan R, Wong PW, Gage PJ, Sieving PA, Ayyagari R. Characterization of mouse orthologue of ELOVL4: genomic organization and spatial and temporal expression. *Genomics*. 2004;83:626–635.
23. Ambasudhan R, Wang X, Jablonski MM, et al. Atrophic macular degeneration mutations in ELOVL4 result in the intracellular misrouting of the protein. *Genomics*. 2004;83:615–625.
24. Lagali PS, Liu J, Ambasudhan R, et al. Evolutionarily conserved ELOVL4 gene expression in the vertebrate retina. *Invest Ophthalmol Vis Sci*. 2003;44:2841–2850.

25. Karan G, Yang Z, Howes K, et al. Loss of ER retention and sequestration of the wild-type ELOVL4 by Stargardt disease dominant negative mutants. *Mol Vis*. 2005;11:657–664.
26. Aveldano MI, Sprecher H. Very long chain (C24 to C36) polyenoic fatty acids of the n-3 and n-6 series in dipolyunsaturated phosphatidylcholines from bovine retina. *J Biol Chem*. 1987;262:1180–1186.
27. Aveldano MI. Phospholipid species containing long and very long polyenoic fatty acids remain with rhodopsin after hexane extraction of photoreceptor membranes. *Biochemistry*. 1988; 27:1229–1239.
28. Schneiter R, Hitomi M, Ivessa AS, Fasch EV, Kohlwein SD, Tartakoff AM. A yeast acetyl coenzyme A carboxylase mutant links very-long-chain fatty acid synthesis to the structure and function of the nuclear membrane-pore complex. *Mol Cell Biol*. 1996;16:7161–7172.
29. McMahon A, Jackson SN, Woods AS, Kedzierski WA. Stargardt disease-3 mutation in the mouse Elovl4 gene causes retinal deficiency of C32-C36 acyl phosphatidylcholines. *FEBS Lett*. 2007;581:5459–5463.
30. Anderson RE, Maude MB, Bok D. Low docosahexaenoic acid levels in rod outer segment membranes of mice with rds/peripherin and P216L peripherin mutations. *Invest Ophthalmol Vis Sci*. 2001;42:1715–1720.
31. Anderson RE, Maude MB, McClellan M, Matthes MT, Yasumura D, LaVail MM. Low docosahexaenoic acid levels in rod outer segments of rats with P23H and S334ter rhodopsin mutations. *Mol Vis*. 2002;8:351–358.
32. Anderson RE, Sieving PA, Maude MB, Naash MI. Mice with G90D rhodopsin mutations have lower DHA in rod outer segment membranes than control mice. In: Anderson RE, LaVail MM, eds. *New Insights into Retinal Degenerative Diseases*. New York: Plenum Press; 2001:235–245.

Investigative Ophthalmology & Visual Science